Melting of a two-dimensional binary cluster of charged particles confined in a parabolic trap

INSTITUTE OF PHYSICS PUBLISHING JOURNAL OF PHYSICS: CONDENSED MATTER

J. Phys.: Condens. Matter **18** (2006) 9385–9401 doi:10.1088/0953-8984/18/41/006

Melting of a two-dimensional binary cluster of charged particles confined in a parabolic trap

W P Ferreira[1], F F Munarin[1], G A Farias[1] and F M Peeters[2]

[1] Departamento de Física, Universidade Federal do Ceará, Caixa Postal 6030, Campus do Pici, 60455-760 Fortaleza, Ceará, Brazil
[2] Department of Physics, University of Antwerp, Groenenborgerlaan 171, B-2020 Antwerpen, Belgium

E-mail: wandemberg@fisica.ufc.br and francois.peeters@ua.ac.be

Received 22 March 2006, in final form 6 September 2006
Published 29 September 2006
Online at stacks.iop.org/JPhysCM/18/9385

Abstract

Melting of a finite size binary system consisting of two types of particles having different charges and/or masses, confined in a two-dimensional (2D) parabolic trap, is studied. The melting temperature is obtained for different values of the ratio between the charges and/or masses of the two types of particles. The two types of particles melt at different temperatures; e.g., particles with smaller charge melt first. The importance of the commensurate/incommensurate configurations and the different normal modes to the melting phenomenon is studied. When the ground state consists of a nonsymmetric arrangement of particles new thermally induced structural phase transitions are found. In addition, a remarkable temperature induced spatial separation of the two types of particles is found.

(Some figures in this article are in colour only in the electronic version)

1. Introduction

Two dimensional (2D) clusters of confined charged particles have been used to model a large number of different experimental systems, such as surface electrons on a thin liquid helium film [1, 2], colloidal suspensions on an inert substrate [3], dusty plasmas [4, 5], and electrons confined in low dimensional semiconductor structures [6]. Even several model systems were recently realized experimentally, consisting of macroscopic objects such as charged metallic balls [7] and magnetic discs [8, 9]. Such 2D clusters exhibit remarkable and unexpected physical behaviour, which is, in most cases, very distinct from the analogue 3D case. As an example, we can cite the microscopic theory of Kosterlitz–Thouless–Halperin–Nelson–Young for phase transition in a 2D system. In the 2D case, and as pointed out by several authors, the transition from a solid phase to a complete isotropic liquid phase can be characterized by a two-step process with an intermediary hexatic phase [10–12]. However, such a melting scenario is

not unique and it depends on the considered system. Furthermore, recent papers have shown that the melting of 2D clusters is nonuniversal [13, 14].

Melting in small clusters of charged particles has also received considerable attention in recent years [15–19]. Very interesting properties have been observed in such systems, e.g. a two-step melting (angular *versus* radial melting) [16], nonhomogeneous melting due to the existence of geometry induced defects [17], and a re-entrant melting behaviour [15, 18] in hard wall confined systems.

In the present paper we investigate the melting phenomenon in a binary system containing two types of particles confined in a parabolic trap. In other words, we study how the presence of impurities [8, 9, 20], represented here by particles with different charges and/or masses, influences the melting of such small confined 2D clusters. The thermal properties of the system are analysed as a function of the ratio between the charges (α) and masses (β) of the two types of particles.

Previously we studied the zero temperature configurations and the normal mode spectrum of such a system as a function of α and β [21]. We found that for distinct values for α (β) the two types of particles separate, and arrange in different shells. In addition, we found that the normal modes are not only determined by the commensurate ratio of the number of particles in the shells, as pointed out in [22], but mainly by the parameters α and β. Melting in such a system was also studied in [22, 23]. However, the results presented in [22] were restricted to the special case in which particles have equal mass and the ratio between the two types of charges was $q_1/q_2 = 2$, while in [23] the special case of two very distinct type of particles, i.e. $q_1/q_2 = 8$, was studied. We extend the work in [22] and investigate the case in which particles have distinct charges and different masses.

Very recently, we addressed the question about the melting in small clusters with one type of particle, but subjected to a Coulomb [24] or to a parabolic [25] confinement potential. Structural phase transitions were found that occur before the complete melting of the system. Recently [19], local melting in small confined clusters of charged particles was observed experimentally. In the present paper, we show how local melting takes place in a binary system of particles with distinct charges and masses. For the computational work we restricted ourselves to the specific system of 13 particles which is representative for the main new physics exhibited by small binary clusters.

The present paper is organized as follows. In section 2 we present the model. The analysis of melting is given in section 3. Our conclusions are presented in section 4.

2. Numerical approach

Our system consists of a two-dimensional cluster with N_f particles with fixed charge q_f and fixed mass m_f, and N_v particles with charge q_v and mass m_v which we will vary. All charged particles interact through a pure repulsive Coulomb potential $1/r$, and the particles are kept together by a parabolic potential. The Hamiltonian of such a system is given by

$$H = \sum_{i=1}^{N_\mathrm{f}} \frac{1}{2} m_\mathrm{f} \omega_0^2 r_i^2 + \sum_{i=1}^{N_\mathrm{v}} \frac{1}{2} m_\mathrm{v} \omega_0^2 r_i^2 + \frac{q_\mathrm{f}^2}{\epsilon} \sum_{i>j=1}^{N_\mathrm{f}} \frac{1}{|\mathbf{r}_i - \mathbf{r}_j|} + \frac{q_\mathrm{v}^2}{\epsilon} \sum_{k>l=1}^{N_\mathrm{v}} \frac{1}{|\mathbf{r}_k - \mathbf{r}_l|} + \frac{q_\mathrm{f} q_\mathrm{v}}{\epsilon} \sum_{m=1}^{N_\mathrm{f}} \sum_{n=1}^{N_\mathrm{v}} \frac{1}{|\mathbf{r}_m - \mathbf{r}_n|}, \tag{1}$$

where ϵ is the dielectric constant of the medium the particles are moving in, and $r_i \equiv |\mathbf{r}_i|$ is the distance of the ith particle from the centre of the confinement potential. In order to reveal the important parameters of the system, it is convenient to define $q_\mathrm{v}/q_\mathrm{f} = \alpha$, $m_\mathrm{v}/m_\mathrm{f} = \beta$ and to

write the energy and the distances in units of $E_0 = (m_f\omega_0^2 q_f^4/2\epsilon^2)^{1/3}$ and $r_0 = (2q_f^2/m_f\epsilon\omega_0^2)^{1/3}$, respectively. In so doing, the Hamiltonian is reduced to

$$H = \sum_{i=1}^{N_f} r_i^2 + \beta \sum_{i=1}^{N_v} r_i^2 + \sum_{i>j=1}^{N_f} \frac{1}{|\mathbf{r}_i - \mathbf{r}_j|} \times \sum_{k>l=1}^{N_v} \frac{\alpha^2}{|\mathbf{r}_k - \mathbf{r}_l|} + \sum_{m=1}^{N_f}\sum_{n=1}^{N_v} \frac{\alpha}{|\mathbf{r}_m - \mathbf{r}_n|}, \tag{2}$$

and the state of the system is determined now by (α, β) and the number of particles (N_f, N_v). Considering the dimensions of the quantities defined above, the temperature is expressed in units of $T_0 = E_0/k_B$, where k_B is the Boltzmann constant.

The ground state configurations ($T = 0$) of the two-dimensional binary system were obtained with the Monte Carlo (MC) method (using the standard Metropolis algorithm [26]) and the modified Newton method [27]. The negatively charged particles are initially put in random positions within some circular area and then allowed to reach a steady state configuration after about 10^4–2×10^5 simulation steps. Simultaneously, we calculated the frequencies of the normal modes of the system using the Householder diagonalization technique [27]. The configuration was taken as final when all frequencies of the normal modes were positive and the energy did not decrease further. Also special care was taken (see [21]) that we started from the ground state configuration and not from a metastable state.

To study melting the system was heated up (where temperature was increased by steps of δT, typically $\approx 10^{-3}$) and equilibrated at the new temperature during 5×10^4–2×10^5 MC steps (one MC step corresponds with a displacement of all particles). After annealing, the average energy is calculated, together with the mean squared radial displacement

$$\langle u_R^2 \rangle \equiv \frac{1}{N} \sum_{i=1}^{N} (\langle r_i^2 \rangle - \langle r_i \rangle^2)/\rho^2, \tag{3}$$

where ρ is the average distance between the particles at zero temperature. The symbol $\langle\ \rangle$ stands for an average over typically 10^6–10^7 MC steps after equilibration of the system.

Angular melting is studied using the angular intrashell displacements,

$$\langle u_{a1}^2 \rangle \equiv \frac{1}{N_s} \sum_{i=1}^{N_s} [\langle (\varphi_i - \varphi_{i1})^2 \rangle - \langle (\varphi_i - \varphi_{i1}) \rangle^2]/(\varphi_0^s)^2, \tag{4}$$

where i_1 indicates the nearest neighbour in the same shell and $\varphi_0^s = 2\pi/N_s$. The angular order between adjacent shells is characterized by the angular intershell displacement, defined as

$$\langle u_{a2}^2 \rangle \equiv \frac{1}{N_s} \sum_{i=1}^{N_s} [\langle (\varphi_i - \varphi_{i2})^2 \rangle - \langle (\varphi_i - \varphi_{i2}) \rangle^2]/(\varphi_0^s)^2, \tag{5}$$

where i_2 indicates the nearest neighbour in an adjacent shell. The shells, as well as all neighbours, were identified at the beginning of each temperature run.

The melting temperature was determined through a Lindemann-like criterion, which has been widely used for 2D finite size clusters. For finite systems, melting occurs over some temperature range and consequently there is some arbitrariness when defining a melting temperature. But what is essential is that fluctuations in the position of the particles change rapidly with temperature beyond some melting temperature. The Lindemann-like criterion adopted in the present work states that melting occurs when the parameters $\langle u^2 \rangle$ defined above reach 0.1 [28], or 0.05 for each coordinate separately. However, this criterion is not unique. A very interesting discussion about melting in small clusters is made in [19].

3. Melting

In this section we present the temperature dependence of the mean square displacements previously defined. First, the general properties of the melting transition will be addressed.

The results presented here were obtained for the particular cluster with $N_f = 7$ particles of fixed charge and with $N_v = 6$ particles of variable charge. This particular choice allows us to compare the melting phenomenon in commensurate and incommensurate configurations simply by changing the ratio α between the charges of the two types of particles [21]. A commensurate configuration occurs when the number of particles in the shells is multiple. If this is not the case, the ring-like configuration is said to be incommensurate. For example, a cluster with 13 particles arranged in shells (rings) as (1, 6, 6), i.e., one particle at the centre, six particles in the first shell, and six particles in the most external shell, presents a commensurate configuration. On the other hand, a cluster with the structural arrangement (1, 5, 7) has an incommensurate configuration. Concerning the lowest normal mode at $T = 0$, the results presented in [21] indicate that such a mode depends on the ratio between charges. Here, we will show that the shape of the mode plays an important role in the melting process. In spite of the particular system chosen here, the general features of the rich melting behaviour presented in this paper remain valid for other clusters.

3.1. Particles with distinct charges

In this section we take by default $\beta = 1$, i.e. we consider particles with the same mass. In this way, the effects of the electrostatic interaction between the different types of particles on the melting phenomenon can be emphasized.

In figure 1(a) the mean radial displacement ($\langle u_R^2 \rangle$) for the cluster with ($N_f = 7$, $N_v = 6$) particles is shown. The ratio between the charges is $\alpha = 3.0$. For these specific values of the parameters (α, β), particles arrange themselves in the commensurate ground state configuration (1, 6, 6), as shown in the inset of figure 1(a). As shown in [21], when particles are arranged in a ring-like structure, the ones with larger charge are always located at the exterior boundary of the system. The melting phenomenon in such a system presents an interesting anisotropy with respect to the different type of particles, i.e., with respect to the charges of the particles. As can be observed in figure 1(a), particles with smaller charge have a smaller radial melting temperature T_r when compared to the ones with larger charge. In general, the internal particles always melt first and such a behaviour was observed for all values of α.

The angular disorder in each shell is analysed through the mean angular intrashell displacements ($\langle u_{a1}^2 \rangle$). Due to the commensurate arrangement of the particles observed in the cluster with ($N_f = 7$, $N_v = 6$) particles, the intrashell melting temperature T_{a1} for the first shell is only slightly smaller than the one for the radial melting (figure 1(b)). Note that the sudden increase in $\langle u_{a1}^2 \rangle$ occurs at the same temperature as the one for the quantity $\langle u_R^2 \rangle$ but the value 0.05 is reached at a different temperature, i.e. $T_{a1} \approx 0.022$ and $T_r \approx 0.024$. The very packed configuration of the cluster generates a high potential barrier for intrashell disorder. However, we found that such a feature is nonuniversal in the binary system, and depends strongly on the interaction between the particles, and consequently on the parameter α.

As already observed in small clusters with only one type of particles [16, 19, 27], the first melting process which takes place in the cluster is characterized by intershell rotation, which is activated at a temperature smaller than the one for radial melting. In figure 1(c), the mean angular intershell displacement ($\langle u_{a2}^2 \rangle$) is shown as a function of temperature. It is clear that the thermal threshold ($T_{a2} \approx 0.012$) for intershell rotation between the two types of particles occurs at a smaller temperature than the one for radial and intrashell melting (figure 1(c)), i.e., $T_{a2} < T_r$ and $T_{a2} < T_{a1}$. As will be shown later, thermally activated intershell rotation is not always observed in a binary system.

Recently, Drocco *et al* [22] found that the matching between the configurations of the particles in the inner and in the outer shell results in a higher melting temperature and in a

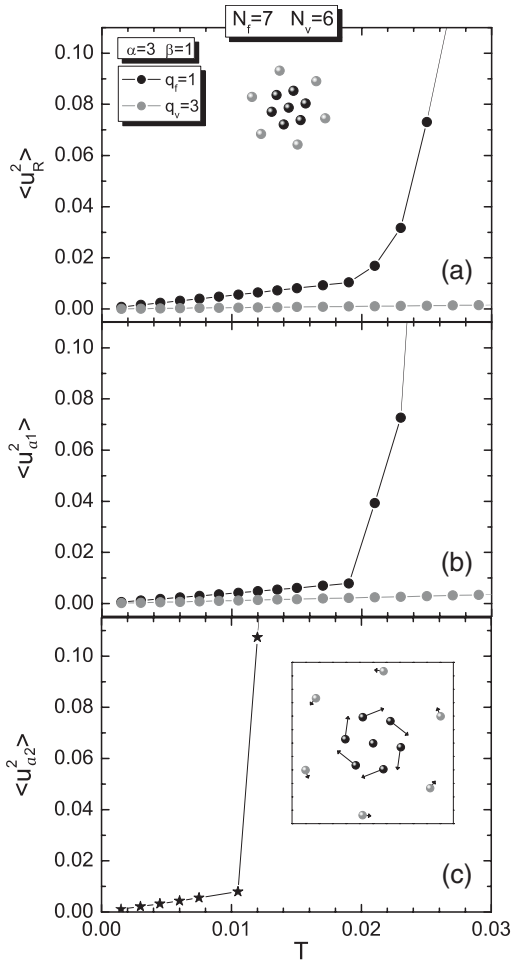

Figure 1. (a) The mean radial displacement ($\langle u_R^2 \rangle$), (b) the mean angular intrashell displacements ($\langle u_{a1}^2 \rangle$), and (c) the mean angular intershell displacements ($\langle u_{a2}^2 \rangle$) for a cluster with $N_\mathrm{f} = 7$, $N_\mathrm{v} = 6$ particles. The ground state configuration is shown in the inset of (a). The black spheres are the reference particles ($q_\mathrm{f} = 1$), while the grey spheres represent the particles with charge $q_\mathrm{v} = 3$. The lowest normal mode is depicted in the inset of (c).

higher thermal threshold for intershell rotation than in the case of nonmatching configurations. These authors only addressed this question with respect to the number of particles in the shells. But, the matching is also a consequence of the effective potential due to the particles in the different shells, and this potential depends not only on the number of particles, but also on other parameters such as the charge and the mass of the particles. Recently, we found that not only the number of particles, but also the ratio between the charges and/or masses of the two types of particles are important parameters in the activation of some specific normal modes at $T = 0$ [21]. Since the normal modes (specially the one associated with the lowest nonzero frequency) are directly related to the stability and deformability of the cluster configuration, they may also be important to the melting transition. As pointed out by Schweigert and Peeters, the melting temperature can, in fact, be written as a function of the frequencies of the normal modes at $T = 0$ [27]. In general, we find here (see also [17]) that the lowest normal mode

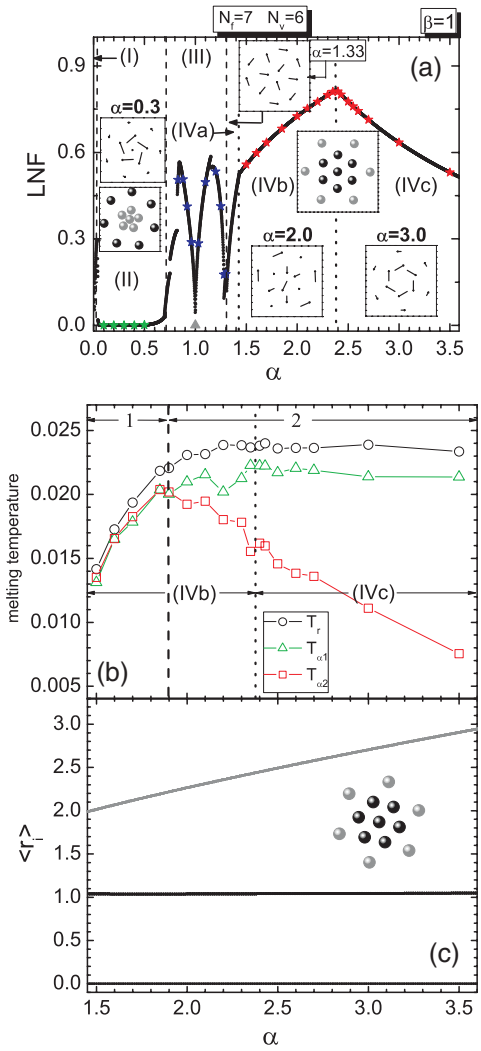

Figure 2. (a) The lowest non-zero frequency (LNF) as a function of α for a cluster with $N_{\rm f} = 7$ and $N_{\rm v} = 6$ particles. Some ground state configurations are shown as the inset (black symbols represent particles with charge $q_{\rm f} = 1$, while grey symbols are for the particles with charge $q_{\rm v} = \alpha$). (b) The radial melting temperature $T_{\rm r}$, the intrashell melting temperature T_{a1} (for the internal shell), and the intershell melting temperature T_{a2} as a function of α. (c) Distance of each particle from the centre of the confinement potential as a function of α. Black and grey curves are associated with the particles with charges $q_{\rm f} = 1$ and $q_{\rm v} = \alpha$, respectively.

plays an important role in the melting process of the binary system. More specifically, an α-dependence of the radial melting temperature is observed when specific lowest normal modes are found at $T = 0$. The thermally activated intershell rotation is also a function of α. In order to illustrate these statements, we resort again to the cluster with $N_{\rm f} = 7$ and $N_{\rm v} = 6$ particles, but now for different values for α.

In order to better understand the results, we first present in figure 2(a) the lowest normal mode frequency (LNF) for the cluster with $N_{\rm f} = 7$, $N_{\rm v} = 6$ particles as a function of α. As discussed above, and as shown previously [21], the lowest normal mode (at $T = 0$) of the binary

system is a sensitive function of the ratio between the charges of the two types of particles. This fact is highlighted in 2(a). The regions I, II, III, and IV define the α intervals where the ground state configurations have different symmetries. Some of the configurations are shown as insets of figure 2(a). E.g., in region II the particles are arranged in the incommensurate configuration (1, 5, 7), i.e., one particle with variable charge q_v at the centre, five particles with variable charge q_v at the first shell, and seven particles with fixed charge q_f at the last shell. Note that in this case the reference particles ($q_f = 1$) are the external ones, since they have now a larger charge. In region IV the commensurate configuration (1, 6, 6) is observed, and in this case the reference particles are the internal ones.

Since radial melting is anisotropic with respect to the different types of particles, we concentrate here on the results concerning the internal ones, which melt first. The analysis of the results can be better understood if we also define the sub-regions IVa ($1.307 \lesssim \alpha \lesssim 1.431$), IVb ($1.431 \lesssim \alpha \lesssim 2.384$), and IVc ($\alpha \gtrsim 2.384$), where the system has the same configuration, but a different lowest normal mode. In region II and in sub-regions IVa, IVb, and IVc the obtained lowest normal modes are shown as insets to figure 2(a). In particular, note that in regions IVb and IVc the observed lowest normal modes consist of a vortex–antivortex pair and intershell rotation, respectively.

The different melting temperatures (T_r, T_{a1}, T_{a2}) for the internal particles as a function of α are shown in figure 2(b) for the cluster with $N_f = 7$, $N_v = 6$ particles. Since we want to investigate the influence of the type of lowest normal mode on the melting process, we will choose the values of α in region IV of figure 2(a), where the cluster presents the same ground state configuration, but distinct lowest normal modes. Note that the vertical dotted line in figure 2(b) separates subregions IVb and IVc previously defined in figure 2(a).

In general, the melting process in the binary system can be characterized by the loss of order between the shells (thermally activated intershell rotation), by the loss of order within a shell (intrashell disorder), and by the radial diffusion of particles among shells (radial melting). The occurrence of the last two kinds of disorder is observed for any value of α in region IV, as can be seen in figure 2(b). On the other hand, thermally activated intershell rotation is not always present, as shown in figure 2(b). E.g., note that for $\alpha \lesssim 1.9$ (region 1—left of the vertical dashed line) the melting temperature for intrashell disorder (green curve with open triangles) is slightly smaller than the one for thermally activated intershell rotation (red curve with square symbols), i.e. $T_{a1} \lesssim T_{a2}$. This means that orientational disorder between shells is observed simply as a consequence of the angular disorder in the internal shell.

Thermally activated intershell rotation is found only for $\alpha \gtrsim 1.9$ (region 2—right of the vertical dashed line). Note that in this interval $T_{a1} > T_{a2}$, implying that the angular disorder between shells occurs before the loss of order within the internal shell. In region 2, T_{a2} continuously decreases with increasing α, indicating that the thermally activated intershell rotation is independent of the lowest normal mode, since no special feature in the curve T_{a2} is observed when the lowest normal mode is changed from a vortex–antivortex to intershell rotation. However, the α-dependence of T_{a2} indicates that thermal activation of intershell rotation becomes easier with increasing α. Such a behaviour can be understood if we analyze the mean distance of each particle from the centre of the confinement potential ($\langle r_i \rangle$) as a function of α, which is shown in figure 2(c). Notice that the radius of the internal shell (particles with charge $q_f = 1$) is practically constant, while the radius of the external shell (particles with charge $q_v = \alpha$) increases with increasing α, which is due to the larger electrostatic repulsion. The larger separation between the shells results in a weaker coupling between them, and consequently makes thermal excitation of intershell rotation easier.

Now we will discuss the radial melting and the thermally activated angular disorder within the shell as a function of α. As commented before, such melting processes were observed for

all values of α in region IV of figure 2(a). Here, we stress again that the results for $T_{\rm r}$ and T_{a1} are associated with the particles in the internal shell, which melt first. The behaviour of the melting temperatures $T_{\rm r}$ and T_{a1} as a function of α suggests that the lowest normal mode has some influence on them (see figure 2(b)). In region IV(b) of figure 2(b), where the lowest normal mode at $T = 0$ is the vortex–antivortex pair (region VI(b)), both temperatures ($T_{\rm r}$ and T_{a1}) are clearly affected by α. More specifically, $T_{\rm r}$ and T_{a1} increase with increasing α up to $T_{\rm r} \approx 0.024$ and $T_{a1} \approx 0.022$, respectively ($\alpha \approx 2.38$). For $\alpha \gtrsim 2.38$ the melting temperatures $T_{\rm r}$ and T_{a1} decrease very slowly with increasing α, where the lowest normal mode at $T = 0$ corresponds to intershell rotation (region VI(c)).

The preceding results suggest that the shape of the lowest mode excitation determines its thermal behaviour. The usual two-step melting found before [16] in clusters with one type of particles is not always found in a binary system. Such a dependence of the melting temperatures on the lowest normal mode was never found before in small confined clusters of charged particles.

The results for the melting temperatures shown in figure 2(b) were restricted to values of α in region IV of figure 2(a), where the ground state configuration is a commensurate state. Now we will study the thermal behaviour of the system in region II ($0.053 \lesssim \alpha < 0.694$) when an incommensurate arrangement of particles is found as the ground state (see inset of figure 2(a)). Note that particles with charge $q_{\rm f} = 1$ are now located at the external shell (black spheres). The incommensurate ground state configuration is a ring-like structure (1, 5, 7).

As already shown by Schweigert and Peeters [27] for a system with one type of particle, and by Ferreira *et al* [21] for the present binary system, incommensurate configurations are highly unstable against intershell rotation. As pointed out by Ferreira *et al*, it is expected that such an instability should also be observed with respect to the structure inside each shell, and with respect to the diffusion of particles between shells, when the temperature of the system is increased [21]. Recently, Drocco *et al* [22] showed that incommensurate configurations have a smaller thermal threshold for intershell rotation as compared to the case of matching configurations. However, the results presented in [22] were restricted to the case $\alpha = 2$. In the present work, we show that the results of [22] are also valid for different values of α. In addition, we show the dependence of the melting temperatures $T_{\rm r}$ and T_{a1} (for incommensurate configurations) on the ratio between the charges of the two types of particles.

The melting temperatures $T_{\rm r}$ and T_{a1} as a function of α are shown in figure 3 for the case of an incommensurate configuration. As can be observed, $T_{\rm r}$ and T_{a1} are one order of magnitude smaller than the melting temperatures found in the case of commensurate configurations (see figure 2(b)). These results mean that not only the thermal activation for intershell rotation, but also the radial melting and the intrashell disorder, are more easily driven in the case of incommensurate configurations. These results are valid for different values of α. Figure 3 also indicates that $T_{\rm r}$ and T_{a1} increase with increasing α. Such a behaviour should be associated with the increase of the coupling between the different types of particles when α increases, and with the height of the saddle point energy separating the ground state from metastable states, as can be seen in figure 3, where the energy difference between the first metastable state (with configuration (6, 7)—see inset in figure 3) and the ground state ($E_{\rm m} - E_{\rm g}$) is shown. The increase of the melting temperature as a function of α follows the increase of ($E_{\rm m} - E_{\rm g}$). It is worth commenting here that the height of the saddle point energy has no influence on the melting temperature shown in figure 2(b), since only one stable state, the ground state, was observed for those values of α.

Up to now we have limited the discussion to the particular cluster with $N_{\rm f} = 7$, $N_{\rm v} = 6$ particles. We found that the effect of the commensurability of the ground state configuration on the melting process of binary systems is also observed in clusters with different number of

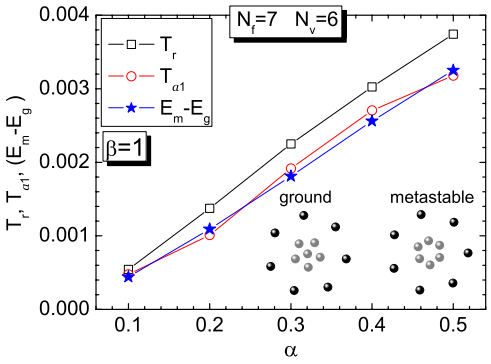

Figure 3. The radial melting temperature $T_{\rm r}$, the intrashell melting temperature T_{a1} (both for the internal shell), and the energy difference between the first metastable state and the ground state ($E_{\rm m} - E_{\rm g}$) as a function of α for the cluster with $N_{\rm f} = 7$ and $N_{\rm v} = 6$ particles. The configurations of the ground state and the metastable state are shown in the inset.

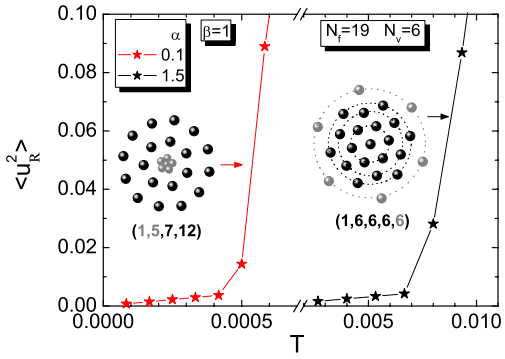

Figure 4. The mean radial displacement ($\langle u_R^2 \rangle$) as a function of the temperature T for commensurate and incommensurate configurations of the cluster with $N_{\rm f} = 19$, $N_{\rm v} = 6$ particles. The ground state configurations are presented as insets. Black spheres represent the reference particles ($q_{\rm f} = 1$), while grey spheres are the particles with variable charge $q_{\rm v} = 0.1$ or $q_{\rm v} = 1.5$.

particles. For example, the temperature dependence of the mean squared radial displacement as a function of temperature for the internal particles of the cluster with $N_{\rm f} = 19$, $N_{\rm v} = 6$ particles is shown in figure 4. This system can present a commensurate or an incommensurate configuration depending on the value of α (see insets in figure 4). As can be observed, the melting temperature for the incommensurate configuration ($\alpha = 0.1$) is one order of magnitude smaller than the one for the matching configuration ($\alpha = 1.5$). For the incommensurate configuration (1, 5, 7, 12), we consider as internal particles only the ones with variable charge (grey spheres), which form the first shell. For the commensurate configuration (1, 6, 6, 6, 6), we considered as internal particles the ones with fixed charge (black spheres), which are distributed over three circular shells. The reason for these choices is the anisotropy in the melting process with respect to the different types of particles as shown previously in figure 1. As can be observed in figure 5(a), for the commensurate configuration, and in figure 5(b), for the incommensurate configuration, the mean squared radial displacement for the external particles is much smaller than the one for the internal particles. In addition, we observe in figure 5(a) that the more internal the shell the smaller the melting temperature.

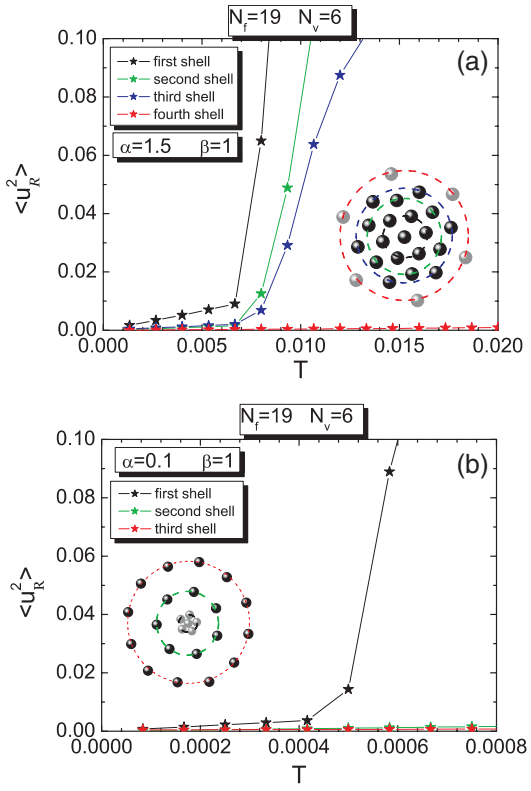

Figure 5. The mean radial displacement ($\langle u_R^2 \rangle$) as a function of temperature for the different shells of the (a) commensurate and (b) incommensurate configurations of the cluster with $N_f = 19$, $N_v = 6$ particles. Ground state configurations are presented as insets. Black spheres represent the reference particles ($q_f = 1$), while grey spheres represent particles with variable charge $q_v = 1.5$ in (a) and $q_v = 0.1$ in (b).

3.2. Particles with distinct masses

In this section we present the results for the case in which particles have different masses, i.e. $\beta \neq 1$, and as an example we take again the cluster with $N_f = 7$ and $N_v = 6$ particles. New commensurate and incommensurate configurations are obtained by changing β.

In figures 6(a)–(c) the dependence of the mean radial displacement ($\langle u_R^2 \rangle$), the mean angular intrashell displacement ($\langle u_{a1}^2 \rangle$), and the mean angular intershell displacements ($\langle u_{a2}^2 \rangle$) are shown, respectively, as a function of temperature in the representative case $\beta = 0.1$, where one type of particle (with mass m_f) is ten times heavier than the other one (with mass m_v). In order to emphasize the inertial effects on the melting properties of the system, we take $\alpha = 1$, i.e. particles with the same charge. The ground state configuration of the system is a commensurate ring-like structure (1, 6, 6), as shown in the inset of figure 6(a). Particles with larger mass are located at the internal shell, in order to minimize the confinement potential energy (see equation (2)). As observed in the preceding section for particles with distinct charges, an anisotropic melting is also found when particles are distinguished from one another by their masses. As can be nicely seen in figures 6(a) and (b) the internal particles melt first. This is in some sense a surprising result since the internal particles are the heaviest ones, and intuitively we could expect that the motion of such particles requires more energy than the

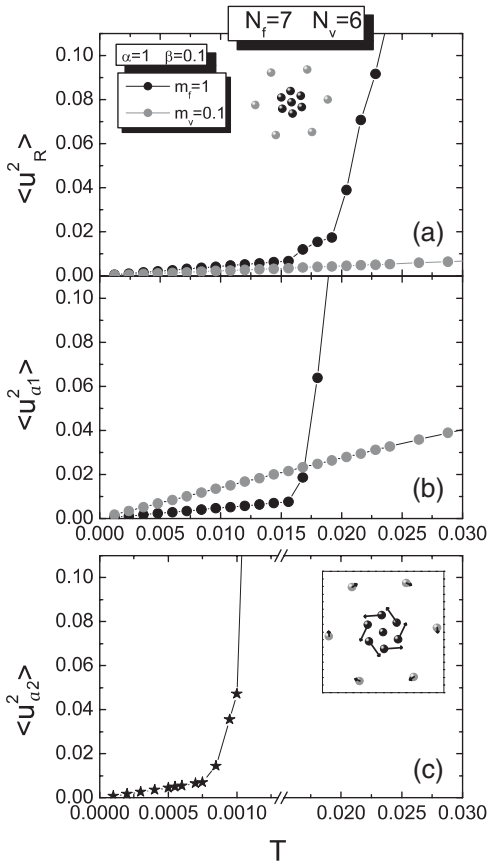

Figure 6. (a) The mean radial displacement ($\langle u_R^2 \rangle$), (b) the mean angular intrashell displacement ($\langle u_{a1}^2 \rangle$), and (c) the mean angular intershell displacements ($\langle u_{a2}^2 \rangle$) for the cluster with $N_\mathrm{f} = 7$, $N_\mathrm{v} = 6$ particles. The ground state configuration is shown in the inset of (a). Black spheres represent the reference particles ($m_\mathrm{f} = 1$), while grey spheres represent the particles with mass $m_\mathrm{v} = 0.1$.

motion of the lighter ones, i.e. a larger temperature is required to destroy the order of the heavier particles. The results presented in figures 6(a) and (b) may be an indication that the inertial properties of the system are not important when compared to the electrical interaction. In fact, we find that the electrostatic interaction between particles overcomes any inertial dependence of the melting process.

In order to verify the importance of the electrostatic effects over the inertial ones, we present in figure 7 the mean radial displacement $\langle u_R^2 \rangle$, for the internal and external shells, as a function of temperature for the cluster with $N_\mathrm{f} = 7$ and $N_\mathrm{v} = 6$ particles, in cases where particles also have different charges, i.e. $\alpha \neq 1$. As previously considered, the reference particles have charge $q_\mathrm{f} = 1$, mass $m_\mathrm{f} = 1$, and are always represented by black spheres, while the other type of particle has charge $q_\mathrm{v} = \alpha$, mass $m_\mathrm{v} = \beta$, and are represented by grey symbols. In general, we find that when $\alpha \neq 1$, and the ring-like structure is the ground state, particles with smaller charge are always located at the internal shell and melt first, independently of the ratio between the masses. This is shown in figures 7(a) and (b) for $\alpha = 0.3$ and $\alpha = 4.85$, respectively, and for three different values of β.

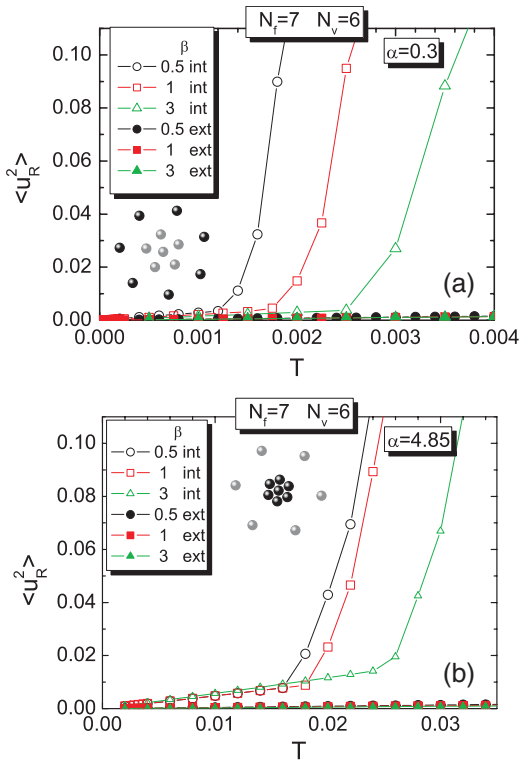

Figure 7. The mean radial displacement $\langle u_R^2 \rangle$ as a function of temperature for the cluster with $N_f = 7$ and $N_v = 6$ particles and for different values of β in the cases where (a) $\alpha = 0.3$ and (b) $\alpha = 4.85$. Typical ground state configurations for each value of α are shown as insets. Black spheres are the reference particles ($m_f = 1$), while grey spheres represent particles with mass $m_v = \beta$.

E.g., in the case ($\alpha = 0.3$, $\beta = 0.5$) we observe that particles with smaller charge and smaller mass (internal ones) melt first. In fact, this is the expected behaviour, since the electrostatic correlation and the inertial effects for these particles are less important than the ones for the reference particles (figure 7(a)). However, the case ($\alpha = 0.3$, $\beta = 3$) shows that the radial melting is mainly determined by the electrostatic correlation effects. Note that particles with smaller charge ($q_v = \alpha$) melt first, even when having larger mass. The larger charge of the reference particles makes the interaction between such particles stronger, which means a more stable structure and a larger melting temperature. The same conclusions are found for the case with $\alpha = 4.85$ (figure 7(b)).

The inertial effects become apparent only when we compare the radial melting temperatures of the internal particles in clusters with the same ratio between charges (α). As can be observed in figures 7(a) and (b), for $\alpha = 0.3$ and $\alpha = 4.85$, respectively, the radial melting temperature of the internal particles increases with increasing mass of such particles. The larger the value of β, the larger the radial melting temperature. Note that such a behaviour is found for commensurate (figure 7(b)) as well as for incommensurate configurations (figure 7(a)). The behaviour observed for the radial melting temperature is also found for angular disorder within the shell (i.e., for the intrashell melting temperature T_{a1}), and for the intershell disorder temperature (T_{a2}).

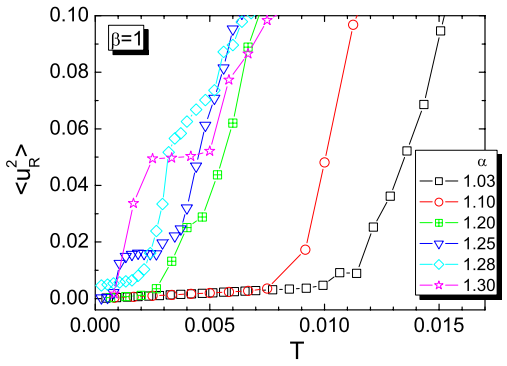

Figure 8. The mean squared radial displacement $\langle u_R^2 \rangle$ as a function of temperature T for a cluster with $N_f = 7$, $N_v = 6$ particles and different values of α. All particles have the same mass, i.e., $\beta = 1$.

3.3. Thermally induced structural phase transitions

Recently, a new feature in the melting of clusters with one type of charged particles was found: namely, the occurrence of local structural phase transitions before complete melting of the system [19, 24, 25]. As shown in [24, 25], these structural transitions depend on the exact ground state configuration of the system and lead to an enhancement of the symmetry of the cluster with increasing temperature. In this section, we show that such structural transitions can also be observed in binary clusters and they produce a segregation of the two types of particle.

As an example, we consider clusters with $\beta = 1$ and values of α in region III of figure 2(a) (indicated by blue stars). In that region, particles of each type are arranged in asymmetric ground state configurations, which are beneficial for observing thermally induced structural phase transitions.

The temperature dependence of the mean squared radial displacement $\langle u_R^2 \rangle$ of the reference particles ($q_f = 1$) is shown in figure 8 for $\alpha = 1.03, 1.1, 1.2, 1.25, 1.28, 1.3$. The mean squared radial displacement for the other particles (with $q_v = \alpha$) is not shown since the values of $\langle u_R^2 \rangle$ are usually one or two orders of magnitude smaller than the ones for the reference particles in the temperature interval considered in figure 8. The radial melting temperatures T_r obtained from figure 8 are comparable to the ones observed in ring-like incommensurate configurations (figure 3), indicating that in both cases the clusters are not very stable.

In figure 8 we notice the occurrence of plateaus for $\alpha = 1.25, 1.28, 1.3$. As shown in [24, 25] for systems with one type of particle, such plateaus are typical signatures for thermal induced structural phase transitions. In order to confirm that this is also the case for the present binary system, we present in figure 9 the temperature dependence of the mean distance of each particle $\langle r_i \rangle$ from the centre of the confinement potential for clusters with $\alpha = 1.03, 1.1, 1.25, 1.3$.

For $\alpha = 1.03$ (figure 9(a)) and $\alpha = 1.1$ (figure 9(b)) the structure of the cluster is changed only when radial melting sets in ($T \approx 0.01$, for $\alpha = 1.03$, and $T \approx 0.009$, for $\alpha = 1.1$). For $\alpha = 1.25$ (figure 9(c)) and $\alpha = 1.3$ (figure 9(d)), thermally induced structural phase transitions are observed at low temperatures. Note that in the considered temperature range, $\langle u_R^2 \rangle$ is still very small, indicating that the oscillations of the particles are not large enough to destroy the ordered structure of the configuration.

Comparing figures 8 and 9 we find that the fast increase of $\langle u_R^2 \rangle$ (in order to form the plateau) is related to structural modifications in the cluster to a more symmetrical configuration.

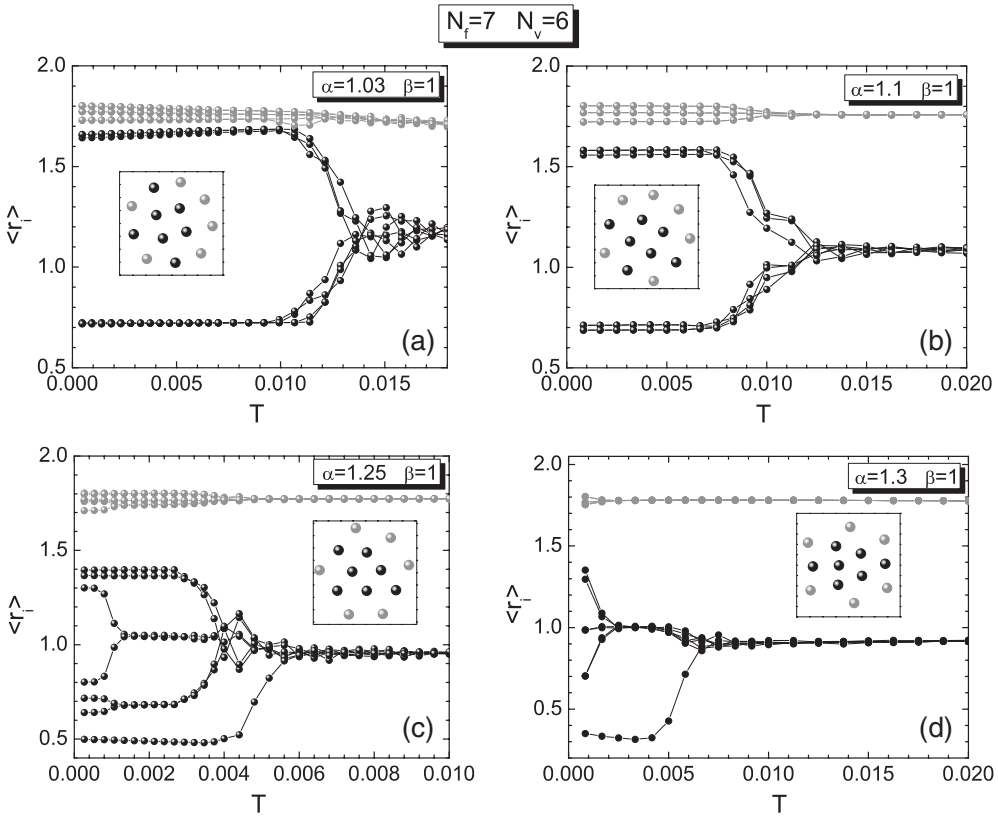

Figure 9. The mean distance of each particle from the centre of the confinement potential as a function of temperature for the cluster with $N_{\rm f} = 7$ and $N_{\rm v} = 6$ particles, and (a) $\alpha = 1.03$, (b) $\alpha = 1.1$, (c) $\alpha = 1.25$, and (d) $\alpha = 1.3$. All particles have the same mass, i.e. $\beta = 1$.

For example, in figure 9(c) a thermally induced structural phase transition occurs at $T \approx 0.001$, which coincides with the beginning of the formation of a plateau in figure 8.

The results in figure 9 also reveal an interesting feature. There is a clear enlargement of the separation between the distinct types of charges with increasing temperature. Particles with smaller charge become more confined in the internal region of the cluster, while the ones with larger charge stay at the edge of the system, and at the same distance from the centre. This *thermally induced charge segregation* is observed for all values of α in region III of figure 2(a), where mixed configurations are found as ground state. The thermally induced charge segregation is observed even when the difference in charge between the particles is very small. E.g., for $\alpha = 1.03$ (figure 9(a)) we observe that after the melting temperature ($T \approx 0.0135$) the mean distance of the reference particles from the centre is $\langle r_i \rangle \approx 1.2$, while for the other ones $\langle r_i \rangle \approx 1.7$. Before melting, both types of particles (see inset of figure 9(a)) are, approximately, at the same distance from the centre of the confinement potential, indicating that the system is in a mixed state as defined in [21]. The thermally induced charge separation is observed for all values of the ratio between the charges.

Now we make some comments about the general behaviour of the melting temperature as a function of α for clusters in region III of figure 2(a). Remarkable features observed in this region are (i) the presence of a large number of metastable states when $\alpha \approx 1$ (see table 1),

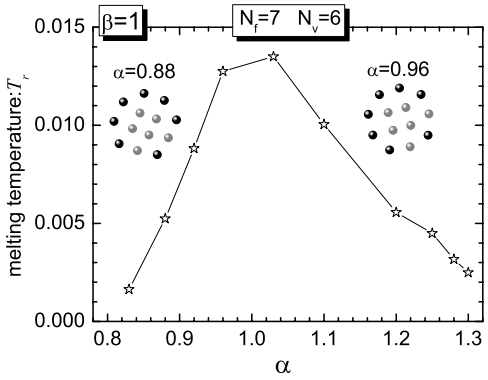

Figure 10. The radial melting temperature T_r as a function of α for the cluster with $N_f = 7$ and $N_v = 6$ particles. Ground state configurations are shown as insets.

Table 1. Number of metastable states (N_{meta}) for several values of the ratio between charges α in clusters with $N_f = 7$, $N_v = 6$ particles.

α	N_{meta}
0.83	72
0.88	109
0.92	108
0.96	109
1.03	112
1.10	115
1.20	84
1.25	40
1.28	34
1.30	18

and, as previously stated, (ii) mixed ground state configurations characterized by an asymmetric distribution of the distinct types of particles. As will be shown here, only the latter has some influence on the melting process.

In figure 10 the radial melting temperature T_r of the cluster with $N_f = 7$, $N_v = 6$ particles as a function of α is shown. The radial melting temperature decreases with increase of the difference $|\alpha - 1|$, i.e. when the difference between charges of both types of particles increases. For $\alpha \approx 1$ the distinct types of particles have almost the same charge, and consequently we have $N_f + N_v = 13$ almost identical particles distributed over rings [16]. When $|\alpha - 1|$ increases, the ring-like structure of the charge distribution is destroyed, since distinct types of particles are found in the same shell. The symmetry breaking in the distribution of charge over the rings reduces the stability of the radial fluctuations of the entire cluster, and consequently the radial melting temperature is reduced.

The stability of the cluster is related to the frequency of the lowest normal mode (LNF). The behaviour of T_r as a function of α (figure 10) does not match the α-dependence of the LNF in region III of figure 2(a). This apparent discrepancy can be easily understood by recalling that for $\alpha \approx 1$ the incommensurate ring-like structure (4, 9) is observed, for which the lowest normal mode is intershell rotation, which does not influence the radial melting temperature. Such incommensurate ring-like structure is highly unstable against the intershell rotation motion, which is reflected in a very small frequency of this mode, that is normally two orders of

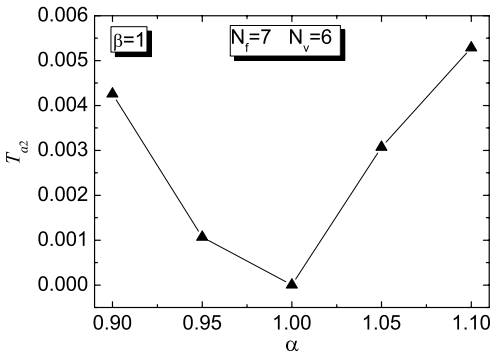

Figure 11. The intershell melting temperature T_{a2} as a function of α for the cluster with $N_{\rm f} = 7$, $N_{\rm v} = 6$ particles in the limit $\alpha \to 1$ in region III of figure 2(a).

magnitude smaller than the frequency of the other modes [27]. Here, the intershell rotation mode has a very small activation frequency $\omega = 6.002 \times 10^{-4}$ for $\alpha = 1$ (grey triangle in figure 2(a)). When α slightly differs from one, the ground state configuration is the same as the one observed for $\alpha = 1$ (see insets in figure 10), and the lowest normal mode is still the intershell rotation, but now with a frequency two orders of magnitude larger than that for the $\alpha = 1$ case.

The α-dependence of the LNF in region III of figure 2(a) is reflected in the intershell melting temperature T_{a2}. In figure 11, we present T_{a2} as a function of α for the cluster with $N_{\rm f} = 7$, $N_{\rm v} = 6$ particles in the limit $|\alpha - 1| \to 0$. Notice that T_{a2} follows the α-dependence of the LNF. For example we found $T_{a2} \backsimeq 10^{-6}$ ($\alpha = 1$), 4×10^{-5} ($\alpha = 0.999$) and 9×10^{-5} ($\alpha = 1.001$). The presence of particles with a larger charge in both rings (for $\alpha \ncong 1$) increases the coupling between such charges and the thermally induced intershell rotation needs higher energy (i.e. higher temperature) to be activated.

4. Conclusions

We studied melting in a binary finite system of charged particles, with distinct charges and/or masses, confined by a parabolic potential. Since the model system presents a large number of parameters (temperature, charge and mass ratio) which have an important influence on the melting properties, we made the choice to present a thorough investigation of a particular cluster with $N = 13$ particles, which exhibits the main features. This particular choice does not restrict the general conclusions and the essential physics of the melting process. E.g., the commensurability effects are general and are not an artefact of the $N = 13$ system.

In general, the binary system exhibits an anisotropic melting with respect to the different types of particles. Particles with smaller charge melt first, and this is observed independently of the mass of both types of particles. The influence of the inertial effect on the melting process becomes relevant only when we compare clusters in which particles have the same charges. In this case, particles with larger mass have the highest melting temperature.

The dependence of the radial ($T_{\rm r}$), intrashell (T_{a1}), and intershell (T_{a2}) melting temperatures on the shape of the lowest normal mode at $T = 0$ was studied for the cases in which particles are arranged in a commensurate ring-like configuration. We found that $T_{\rm r}$ and T_{a1} have different behaviours for distinct shapes of the lowest modes. Thermally activated intershell rotation is not observed for any value of α, which means that the melting process in small clusters of charged particles is not universal.

A remarkable temperature induced separation of the distinct types of particles is observed with increasing temperature. Particles with smaller charge become confined in the internal region of the cluster. This interesting thermal segregation was also observed for particles with different masses.

The opposite limit of the present system is the one in which $N = (N_f + N_v) \to \infty$. In this case, the formation of a 2D Wigner crystal will essentially depend on the ratio N_f/N_v between the number of both types of particles. If it is a nonrational number, it is expected that no Wigner lattice will be formed and the system will be disordered. In the other case, one may expect ordered crystal structures with a larger unit cell (how large will depend on the exact value of the ratio N_f/N_v). Because of the complexity of the situation in 2D we prefer not to speculate on this issue and limit ourselves to the finite size system where we can make clear statements that are supported by our numerical results. The possible $T = 0$ lattice structures and the melting of such a 2D binary system is very interesting and will be left for future study.

Acknowledgments

FFM and GAF were supported by the Brazilian National Research Councils CNPq and CAPES and the Ministry of Planning (FINEP). Part of this work was supported by the Flemish Science Foundation (FWO-Vl).

References

[1] Crandall R S and Williams R 1971 *Phys. Lett.* A **34** 404
[2] Grimes C C and Adams G 1979 *Phys. Rev. Lett.* **42** 795
[3] Golosovsky M, Saado Y and Davidov D 2002 *Phys. Rev.* E **65** 061405
[4] Chu J H and L I 1994 *Phys. Rev. Lett.* **72** 4009
[5] Melzer A 2003 *Phys. Rev.* E **67** 016411
[6] Jacak L, Hawrylak P and Wójs A 1998 *Quantum Dots* (Berlin: Springer)
[7] Saint Jean M, Even C and Guthmann C 2001 *Europhys. Lett.* **55** 45
[8] Grzybowski B A, Stone H A and Whitesides G M 2000 *Nature* **405** 1033
[9] Grzybowski B A, Jiang X, Stone H A and Whitesides G M 2001 *Phys. Rev.* E **64** 011603
[10] Kosterlitz J M and Thouless D J 1973 *J. Phys. C: Solid State Phys.* **6** 1181
[11] Halperin B I and Nelson D R 1978 *Phys. Rev. Lett.* **41** 121
[12] Young A P 1979 *Phys. Rev.* B **19** 1855
[13] Zahn K, Lenke R and Maret G 1999 *Phys. Rev. Lett.* **82** 2721
[14] Branício P S, Rino J P and Studart N 2001 *Phys. Rev.* B **64** 193413
[15] Bubeck R, Bechinger C, Neser S and Leiderer P 1999 *Phys. Rev. Lett.* **82** 3364
[16] Bedanov V M and Peeters F M 1994 *Phys. Rev.* B **49** 2667
[17] Kong M, Partoens B and Peeters F M 2003 *New J. Phys.* **5** 23
[18] Schweigert I V, Schweigert V A and Peeters F M 2000 *Phys. Rev. Lett.* **84** 4381
[19] Coupier G, Guthmann C, Noat Y and Saint-Jean M 2005 *Phys. Rev.* E **71** 046105
[20] Nelissen K, Partoens B and Peeters F M 2004 *Phys. Rev.* E **69** 046605
[21] Ferreira W P, Munarin F F, Nelissen K, Costa Filho R N, Peeters F M and Farias G A 2005 *Phys. Rev.* E **72** 021406
[22] Drocco J A, Olson Reichhardt C J, Reichhardt C and Jankó B 2003 *Phys. Rev.* E **68** 060401(R)
[23] Nelissen K, Partoens B, Schweigert I and Peeters F M 2006 *Europhys. Lett.* **74** 1046
[24] Ferreira W P, Partoens B, Peeters F M and Farias G A 2005 *Phys. Rev.* E **71** 021501
[25] Tomecka D, Partoens B and Peeters F M 2005 *Phys. Rev.* E **71** 062401
[26] Metropolis N, Rosenbluth A W, Rosenbluth M N, Teller A M and Teller E 1953 *J. Chem. Phys.* **21** 1087
[27] Schweigert V A and Peeters F M 1995 *Phys. Rev.* B **51** 7700
[28] Lozovik Yu E and Fartzdinov V M 1985 *Solid State Commun.* **54** 725
Bedanov V M, Gadiyak G V and Lozovik Yu E 1985 *Phys. Lett.* A **109** 289